SUPPLEMENTARY DATA

Supplementary Table 1. Chemical shifts (ppm) and assignments of backbone and side-chain protons of F9A fusion domain in DPC micelles at pH 5.

Residue	HN	Hα	Hβ	Others
G1		3.862		
L2	9.324	4.036	1.639	γCH2, 1.509; δCH3, 0.786, 0.870
			1.623	
F3	8.911	4.176	3.137	2,6H, 7.212
			3.105	
G4	8.476	3.724		
		3.945		
A5	8.159	4.229	1.494	
I6	8.069	3.640	1.899	γCH2, 1.899, 1.012; γCH3, 0.846; δCH3, 0.774
A7	8.416	3.845	1.300	
G8	8.161	3.829		
A9	7.782	4.239	1.444	
I10	7.956	3.700	1.929	γCH2, 1.760, 1.069; γCH3, 0.856; δCH3, 0.767
E11	8.053	4.001	2.085	γCH2, 2.403, 2.277
N12	8.131	4.660	2.794	δNH2, 7.614, 6.886
G13	8.038	3.775		
		3.918		
W14	8.523	4.382	3.311	
E15	8.454	3.873	1.960	γCH2, 2.221
G16	7.884	3.759		
		3.885		
M17	7.879	4.312	2.034	γCH2, 2.420, 2.499
I18	7.695	3.974	1.816	γCH2, 1.289, 1.035; γCH3, 0.755; δCH3, 0.681
D19	8.167	4.491	2.663	
G20	8.264	3.895		

Supplementary Table 2. Statistics of solution structure calculation of F9A fusion domain in DPC micelles at pH 5.

Target function (Å)			0.028 ± 0.003
Experimental NMR constraints			
	NOE		**147**
		Intrasidue	52
		Sequential	48
		Medium Range	47
		Long Range	0
	Angle constraints		**63**
		Phi	23
		Psi	16
		Chi1	12
		Chi2	12
NMR constraint violations			
	NOE constraint violations		
		Sum (Å)	1.95 ± 0.10
		Maximum (Å)	0.17 ± 0.007
	Angle constraint violations		
		Sum (º)	5.73± 2.86
		Maximum (º)	3.95 ± 0.13
Energy (kcal/mol)			–224.9 ± 4.24
Root mean square deviation from mean structure (Å)			
	Backbone atoms of all residues 1-20		0.79±0.40
	Heavy atoms of all residues 1-20		1.35±0.35
	Backbone atoms of residues 1-12		0.10±0.06
	Heavy atoms of residues 1-12		0.89±0.21
	Backbone atoms of residues 14-18		0.19±0.08
	Heavy atoms of residues 14-18		0.94±0.22
Ramadchandran statistics analyzed using PROCHECK-NMR			
	Residues in allowed regions		100%

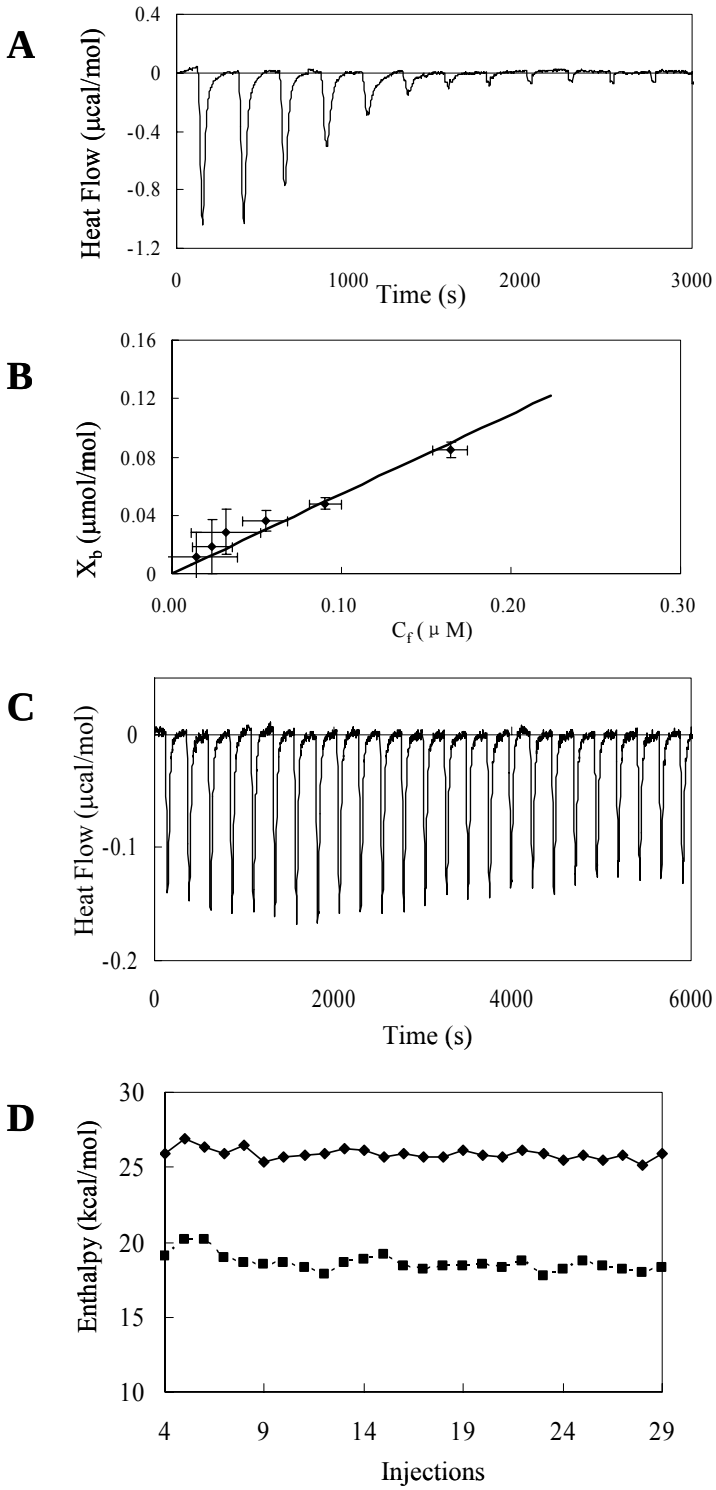

Supplementary Figure S1 Binding of the I10A mutant fusion domain to lipid bilayers composed of POPC:POPG (4:1) by isothermal titration calorimetry. A, Measurement of binding equilibrium by titration of SUVs to I10A fusion domain. B, Binding curve of I10A fusion domain, expressed as mol fraction peptide/lipid bound versus free peptide. C, Measurement of enthalpy of binding by titration of I10A fusion domains to SUVs. D, Reaction enthalpies of fusion domain binding to lipid bilayers. ◆, I10A, ■, F9A_I10A.

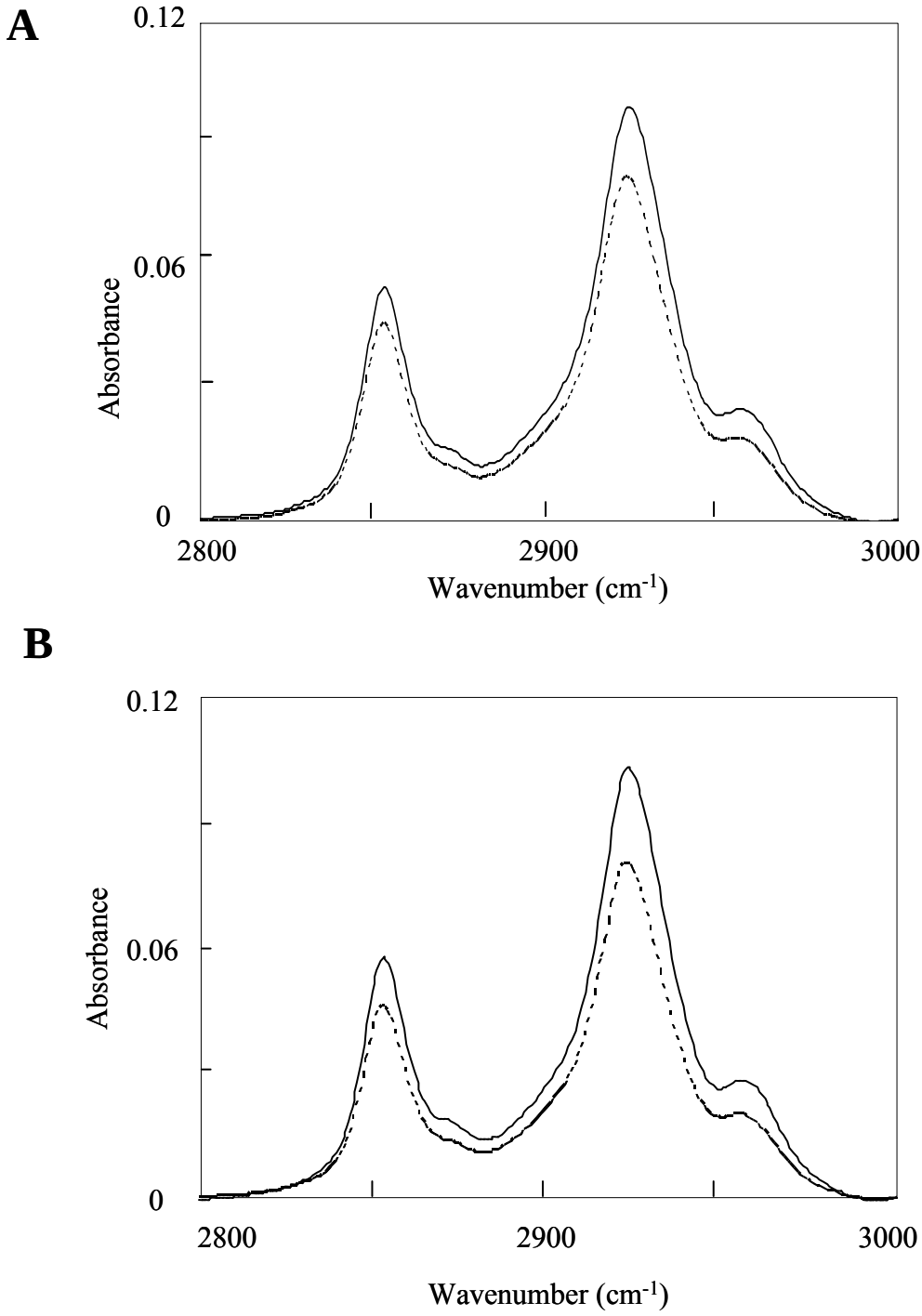

Supplementary Figure S2 Polarized ATR-FTIR spectra of in the methylene stretching region of a DMPC/POPC:POPG (4:1) supported bilayer with 100 μg/ml of I10A (A) or F9A_I10A (B) mutant fusion domains bound. Solid line, spectra recorded with parallel polarized infrared light; dotted line, spectra recorded with perpendicular polarized infrared light.

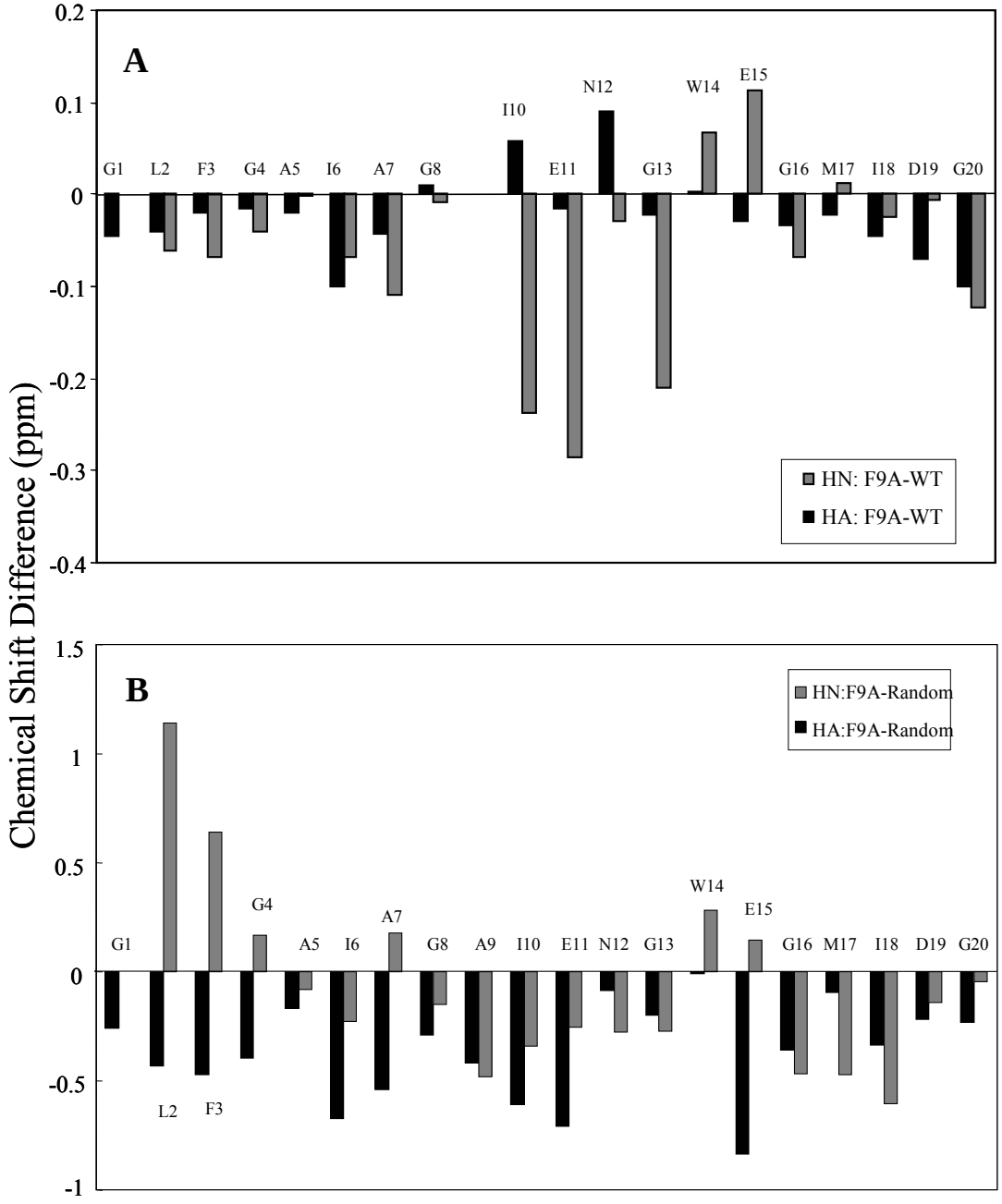

Supplementary Figure S3 Backbone HN and Hα chemical shift differences between the F9A and wild-type fusion domains (A) and between the F9A fusion domain and tabulated chemical shifts of corresponding amino acids in random coil conformation (B).

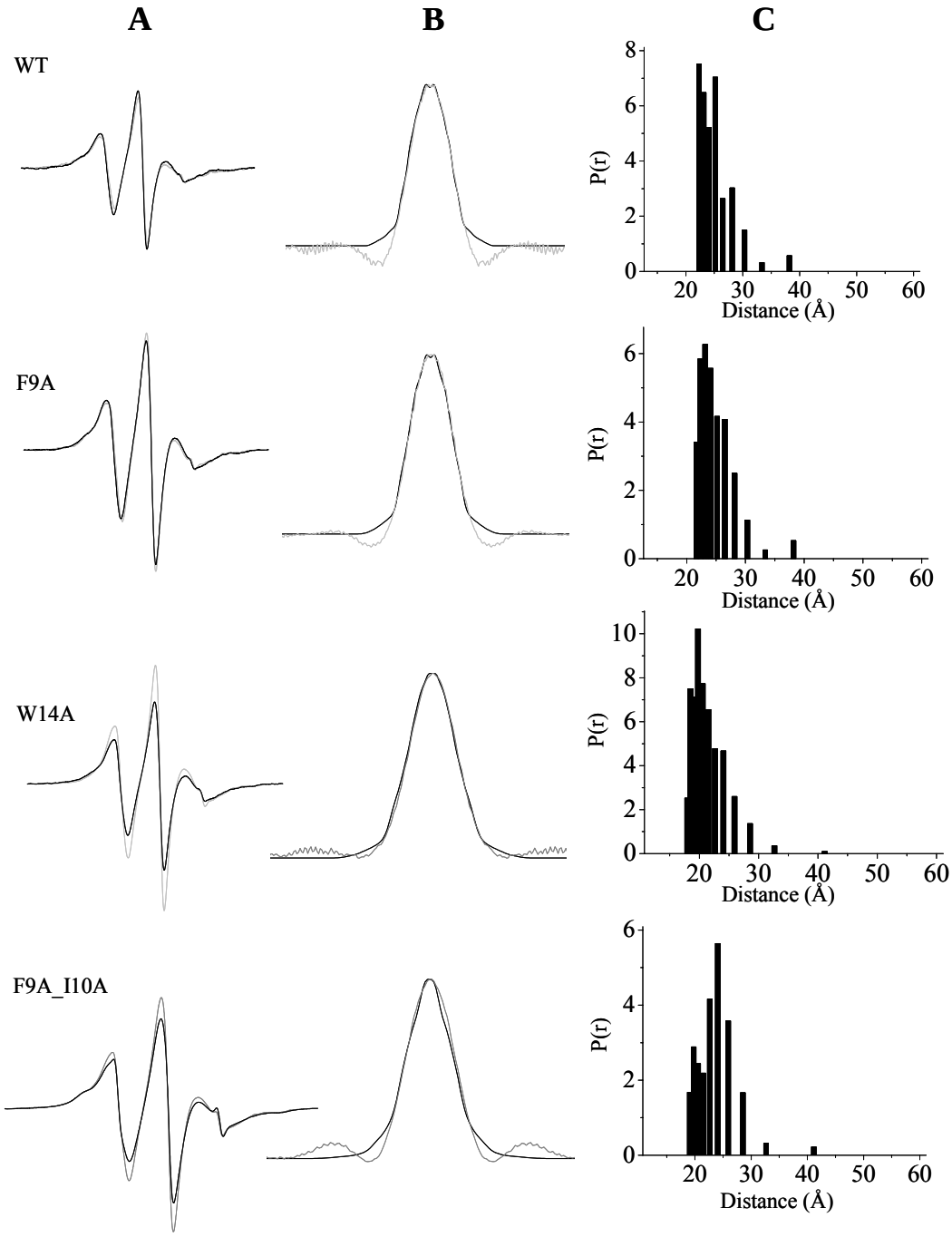

Supplementary Figure S4 Analysis of continuous wave EPR spectra of wild-type, F9A, F9A_I10A and W14A mutant fusion domains in POPC:POPG (4:1) bilayers at pH 5. A, comparison of spectra of the double-labeled domains (black) with and the sum of spectra of the single-labeled domains (gray). B, comparison of the devolution of the double-labeled spectra with the sum of the single-labeled spectra (gray) and the best fit sum of Pake functions (black). C, Distance distributions leading to the best fit sum of the Pake functions.